

# Calibration Changes to Terra MODIS Collection-5 Radiances for CERES Edition 4 Cloud Retrievals

Sunny Sun-Mack, Patrick Minnis, Yan Chen, David R. Doelling, Benjamin R. Scarino, Conor O. Haney, and William L. Smith, Jr.

**Abstract**— Previous research has revealed inconsistencies between the Collection 5 (C5) calibrations of certain channels common to the Terra and Aqua MODerate-resolution Imaging Spectroradiometers (MODIS). To achieve consistency between the Terra and Aqua MODIS radiances used in the Clouds and the Earth's Radiant Energy System (CERES) Edition 4 (Ed4) cloud property retrieval system, adjustments were developed and applied to the Terra C5 calibrations for channels 1-5, 7, 20, and 26. These calibration corrections were developed independently of those used for MODIS Collection 6 (C6) data, which became available after the CERES Ed4 processing had commenced. The comparisons demonstrate that the corrections applied to the Terra C5 data for CERES Edition 4 generally resulted in Terra-Aqua radiance consistency that is as good as or better than that of the C6 datasets. The C5 adjustments resulted in more consistent Aqua and Terra cloud property retrievals than seen in the previous CERES edition. Other calibration artifacts were found in one of the corrected channels and in some of the uncorrected thermal channels after Ed4 began. Where corrections were neither developed nor applied, some artifacts are likely to have been introduced into the Ed4 cloud property record. For example, the degradation in the Aqua MODIS 0.65- $\mu\text{m}$  channel in both the C5 and C6 datasets affects trends in cloud optical depth retrievals. Thus, despite the much-improved consistency achieved for the Terra and Aqua datasets in Ed4, the CERES Ed4 cloud property datasets should be used cautiously for cloud trend studies because of those remaining calibration artifacts.

**Index Terms**—Calibration, climate, cloud, Clouds and the Earth's Radiant Energy System (CERES), Moderate Resolution Imaging Spectroradiometer (MODIS)

## I. INTRODUCTION

THE NASA Clouds and Earth's Radiant Energy System (CERES) is monitoring the Earth's radiation budget and relies on broadband radiances measured by scanners on multiple satellites that are interpreted with the aid of high-

spatial resolution, narrowband spectral radiances taken simultaneously by imagers on the same satellites. The imager data are used to identify the scene as clear or cloudy and to estimate the relevant parameters necessary to characterize the scene, such as surface skin temperature or cloud optical depth. These are used to select the appropriate broadband unfiltering procedure and angular directional models (ADM) for converting the CERES instantaneous unfiltered radiances to outgoing top-of-atmosphere fluxes, to choose the proper directional or diurnal model for estimating the fluxes over the other hours of the day in order to compute daily averaged fluxes, and to calculate from the cloud properties the surface and atmospheric fluxes [1]. By themselves, the cloud properties comprise a climate data record (e.g., [2-4]) and are valuable for evaluating climate models (e.g., [5-7]). To construct reliable climate data records from the CERES measurements, it is critical not only to accurately calibrate the CERES broadband scanners, but also to ensure that the imager calibrations are stable and consistent among the various platforms. Otherwise, calibration-dependent trends or differences can be introduced and produce spurious climate signals.

CERES uses the MODerate-resolution Imaging Radiometer (MODIS) to retrieve cloud properties for the broadband scanners on the Terra and Aqua Sun-synchronous satellites. The MODIS calibration procedures are periodically updated to account for instrument degradation and new information that together improve the calibrations in the level 1B data, which are reprocessed for each collection. Although the MODIS Collection 5 (C5) calibrations have been well characterized and carefully monitored for both Terra and Aqua [8-11], various researchers (e.g., [9, 12, 13, 14]) determined that, in certain channels, there are some significant differences between the radiances measured by the Terra and Aqua MODIS copies, as well as degradation in some channels that was not reflected in the calibration level-1B lookup tables. Such discrepancies can introduce significant differences in certain cloud properties retrieved from Terra and Aqua MODIS data (e.g., [15,16]) and introduce spurious trends. A combination of MODIS Collection 4 (C4) and C5 data was used in the CERES Edition 2 (Ed2) cloud mask and retrievals [13, 17] that are used in the generation of CERES Ed2 and Edition 3 flux products. No significant differences were found in the calibrations of the various channels between the C4 and

Manuscript received December 20, 2017. This work was supported by the Clouds and the Earth's Radiant Energy System Project through the NASA Science Mission Directorate.

S. Sun-Mack, P. Minnis, Y. Chen, B. Scarino, and C. Haney are with Science Systems and Applications, Inc., Hampton, VA 23666 (email:szedung.sun-mack-1@nasa.gov).

W. Smith and D. Doelling are with the Science Directorate, NASA Langley Research Center, Hampton, VA 23681.

C5 versions. Thus, it is concluded that the C4 level-1B radiances had the same Terra-Aqua differences and degradation as their C5 counterparts and the CERES Ed2 cloud properties were affected by those calibration issues throughout the record.

To account for the degradation and other newly found dependencies in some of the instrument components, several improvements were introduced in the MODIS Collection 6 (C6) Level-1B (L1B) radiance calibrations [14, 18]. Release of the C6 L1B data began in 2012 [18]. However, CERES continued to use C5 MODIS radiances until C5 production was stopped in January in 2017. Since February 2017, CERES incorporated the C6 MODIS radiances. Development of the CERES Edition 4 (Ed4) cloud (e.g., [19]) and flux algorithms began long before the C6 data were released and, as such, were geared to using the C5 radiances throughout the record. Thus, the CERES Ed4 cloud algorithms did not have the benefit of the changes made in the development of the C6 L1B products. To overcome some of the known calibration differences, independent methods were developed to normalize the C5 radiances from Terra MODIS to their Aqua counterparts prior to the C6 release. This paper documents the corrections applied to the C5 data used in CERES Ed4, compares the results to the C6 radiances, and discusses some of the implications of the calibrations to the CERES cloud property record.

## II. DATA AND METHODOLOGY

### A. Satellite Data

The CERES project receives a sub-sampled version of the full MOD02 (Terra) and MYD02 (Aqua) MODIS L1B calibrated geolocation dataset. Data from every other pixel and scan line are provided for 19 of the 36 channels. Of those channels, only 12 are used in the cloud analysis, including seven solar reflectance and 5 infrared bands. The C5 L1B lookup tables are used to convert the counts to reflectance  $R$  for the solar reflectance channels and to radiance for the thermal emissive channels. Brightness temperature  $T$  is derived from the thermal radiances using the Planck function applied at the central wavelength of a given channel. The Aqua channels were found to be very stable through 2008 [11,12, 20]. Because of that stability, the Aqua MODIS solar channels were selected to serve as the solar reflectance references for the Global Satellite Inter-Calibration System (GSICS) [21]. They also serve Ed4 as references used to adjust the Terra calibrations for CERES. The Aqua 1.6- $\mu\text{m}$  channel, however, was determined to be too noisy and unreliable for use by CERES, since the majority of the detectors are inoperable [20]. Thus, for consistency, no 1.6- $\mu\text{m}$  data are used for either satellite in CERES Ed4 cloud processing. The 1.24 and 2.13- $\mu\text{m}$  channels are used for cloud detection and secondary cloud particle size retrievals during processing of both the Aqua and Terra data [19].

For CERES Ed4, solar channel data from July 2002 through December 2011 are used to normalize Terra channels to their Aqua counterparts. Determination of calibration changes after 2011 were not continued because of processing

constraints. To evaluate the calibrations, C6 L1B data are used for comparisons with the adjusted Terra C5 reflectances and brightness temperatures.

### B. Solar Channel Normalizations

To effect the normalizations, the Terra and Aqua MODIS data were ray-matched in the same manner used by [22], who employed nadir and off-nadir nearly simultaneous, matched Terra and Aqua reflectances taken within a 15-min window and averaged over the same 50-km region whenever the respective Terra and Aqua viewing zenith angles are the same and the differences between their relative azimuth angles are less than  $7.5^\circ$ . Except for the Terra shortwave infrared channel (SIR, 3.8  $\mu\text{m}$ ), no calibration adjustments were applied for the period 1 July 2000 to 13 May 13, 2002. No adjustments were made for spectral response function differences between the Terra and Aqua bands.

The reflectances provided in the Terra MODIS C5 dataset were altered for three different periods beginning with the launch of Aqua by multiplying the nominal C5 reflectance ( $\rho_{C5}$ ) by the correction factor,  $f_g$ :

$$\rho_{C5'} = f_g * \rho_{C5}, \quad (1)$$

where

$$f_g = a_0 + a_1 * DSL, \quad (2)$$

and  $DSL$  is the number of days since the launch of Aqua, 14 May 2002. No changes were applied prior to 14 May 2002. The adjusted data ( $\rho_{C5'}$ ) are referred to here as Terra C5' data.

The calibration changes are evaluated by comparing matched Terra and Aqua data from days 1, 11, and 21 from each month for 2003, 2008, 2013, 2015, and 2016 to sample segments of each calibration period with special focus on more recent years to detect any degradation. For these comparisons, the Aqua and Terra data were matched using only those data taken within  $\pm 30$  min and  $\pm 10^\circ$  of solar zenith angle  $SZA$ , and in the same  $10^\circ$  and  $30^\circ$  viewing zenith and relative azimuth angle bins, respectively. While these constraints are much looser than those used by [22], they provide a much greater amount of data. The matched datasets include both the original C5 and C5' data as well as Terra MODIS C6 data. The Aqua C6 reflectances are negligibly different from their C5 counterparts, while the magnitudes of the changes to Terra, variable with time and spectral band, are significant in some instances.

### C. Infrared Channel Normalizations

1) *Channel 20, SIR (3.78  $\mu\text{m}$ ):* Comparisons with Aqua MODIS between July 2002 and July 2005 show that the Terra MODIS measures SIR temperatures  $T_{Te}$  almost 0.55 K greater than Aqua during the daytime [13]. Thus, 0.55 K is subtracted during the daytime. During the night,  $T_{Te}$  can be from 1 – 3 K warmer than the Aqua temperature  $T_{Aq}$ , when  $T_{Te} \sim 270$  K up to 15 K warmer at  $T_{Te} \sim 220$  K. The example in Fig. 1 shows a scatterplot of Aqua and Terra SIR temperatures for July 2007 (Fig. 1a) and the corresponding temperature differences between Aqua and Terra,  $T_{Aq} - T_{Te}$ , as a function of  $T_{Te}$ . Such large differences between Aqua and Terra, especially at the

low end, are seen in all MODIS C5 data records during nighttime. Seasonal Terra SIR calibration curves (red line in Fig. 1b) were developed for each year by fitting values of  $T_{Aq} - T_{Te}$  to a Gaussian error function ( $erf$ ) as a function  $T_{Te}$ . The formula used is

$$T_{Aq} = a_0 + a_1 * (\text{erf}(a_2 * (T_{Te} - 209.25))) + a_3 * (T_{Te} - 209.25). \quad (3)$$

where the fitting coefficients  $a_i$  were computed using the matched datasets for each season for each year between July 2002 and August 2011. For application to the Terra data, a lookup table of  $T_{Aq} - T_{Te}$  values, correction addends  $\Delta T(C5')$ , was computed from the results of fitting (1) for each month in the center of each season at a resolution of 1.0 and 0.5 K for  $T_e < 235$  K and  $T_e \geq 235$  K, respectively. Lookup tables for each remaining month between June 2002 and July 2011 was created by linear interpolation between the seasonal center months. For Terra data taken earlier than June 2002, the correction factors for July 2002 – June 2003 are used for the relevant month. Likewise, lookup tables for July 2010 – August 2011 are used for Terra data taken after 31 August 2011.

In practice, the C5' values for Terra channel 20 were computed as follows. If the solar zenith angle  $SZA \leq 82.0^\circ$ ,

$$T_{Te}(C5') = T_{Te}(C5) - 0.55 \text{ K}. \quad (4)$$

Otherwise,

$$T_{Te}(C5') = T_{Te}(C5) + \Delta T(C5'), \quad (5)$$

where the correction factor comes from the appropriate data month lookup table.

2) *Longwave infrared channels*: Li et al. [23] found that the Terra and Aqua MODIS C5 infrared (IR, 10.8  $\mu\text{m}$ ), split window (SWC, 12.0  $\mu\text{m}$ ), and CO2 (13.3  $\mu\text{m}$ ) channels are consistent to  $\pm 0.1$  K through 2012. No differences between daytime and nighttime were reported. No calibration changes were made to Terra for either of these channels. The Terra and Aqua channels 27 (6.7  $\mu\text{m}$ ) and 29 (8.55  $\mu\text{m}$ ) C5 temperatures differ by  $1.0 \pm 0.9$  K and  $1.1 \pm 0.7$  K, respectively (Li et al. 2013). As these differences were unknown prior to development of the Ed4 processing, no changes were made to the Terra calibrations for these channels. Any other differences found between the various channels are noted in the following sections. Comparisons between the Terra and Aqua MODIS longwave infrared channels for C5 and C6 data are performed here using the approach of [22].

### III. COMPARISON OF TERRA AND AQUA CALIBRATIONS

Results are presented for the Terra channels that were adjusted. They are compared with their Aqua C5 counterparts as well as the corresponding Terra C6 data. Because the Aqua C5 and C6 calibrations are so similar, it is assumed that comparisons of Terra with Aqua C5 are essentially the same as comparing with Aqua C6. Thus, Aqua C6 and C5 data are used interchangeably.

#### A. Solar Channels

The calibration adjustment coefficients  $a_0$  and  $a_1$  applied to (2) are listed in Table I for seven Terra MODIS channels. The adjustment factor  $f_g$  is dominated by the first term in (2) of section B; non-zero values for  $a_1$  occur for only a few cases. Values for  $f_g$  range from 0.9706 for channel 5 to 1.043 for channel 26. Very small changes,  $< 1\%$ , are applied to the channel 2 and 7 C5 calibrations. For the most heavily used solar band in the Ed4 daytime algorithms, channel 1 (VIS), the Terra reflectances are raised by 1.0% at the beginning of the Aqua period up to 3.2% after 31 March 2009. These adjustments coincide with the Terra-MODIS solar diffuser door being permanently open beginning in July 2, 2013, and a Terra-MODIS solar diffuser correction applied in early 2009 that resulted in a total degradation of 1.5% [20].

Fig. 2 compares reflectances from Terra C5, Terra C5', and Terra C6 at 0.63 (top) and 1.24  $\mu\text{m}$  (bottom) with matched Aqua C5 data for 11 April 2015. In these figures, the scatter density plots are shown with the line of agreement (black) and the linear fit to the data (red), as well as the statistics of the linear fits forced through the origin. Given the assumption that zero reflectance at 0.000 is true all of the calibrations, the linear fits were performed by forcing the intercept to be (0.000,0.000) for all sets of matched data. This eliminates the impact of a varying intercept on the computed slope, facilitating the analysis of trends in the fits. The slopes range from 0.958 for the C5 pairs (Fig. 2a) to 0.988 for both the C5'-C5 (Fig. 2b) and C6-C5 (Fig. 2c) matches for channel 1 (0.63  $\mu\text{m}$ ) and from 0.994 for C5'-C5 (Fig. 2e) to 1.024 for C5-C5 (Fig. 2d) for channel 5 (1.24  $\mu\text{m}$ ). The C6-C5 1.24- $\mu\text{m}$  slope (Fig. 2f) is midway between the other two. The magnitude of the mean 0.63- $\mu\text{m}$  reflectance differences between Terra C5 and Aqua C5 are an order of magnitude greater than those from the other two combinations. At 1.24  $\mu\text{m}$ , the C5-C5 and C6-C5 differences are 0.017 and 0.012, respectively, and are noticeably greater than the 0.005 C5'-C5 difference. The standard deviations of the differences are essentially the same for all cases. These types of comparisons between Aqua and Terra were made using data from days 1, 11, and 21 from each month for 2003, 2008, 2013, 2015, and 2016 to sample segments of each calibration period with special focus on more recent years to detect any degradation.

Fig. 3 shows the results for the channel-1 data. The C5-C5, C5'-C6, and C6-C6 values are indicated in blue, red, and green, respectively. Slopes and reflectance differences for each day are presented in Figs. 3a and 3c, respectively. Both quantities show a fairly systematic annual cycle that tends to a maximum around the beginning of each year and bottoming out late during each year. This seasonal "cycle" most likely reflects the varying angular configurations of the matched datasets, as well as the changing surface types viewed in the matching zones. The matches occur only over polar regions. During the beginning of the year, most of the matches are in the Southern Hemisphere near or over Antarctica, while the middle of the year is dominated by scenes over the Arctic. In addition to the annual cycle of viewed geography, it is probable that the angular differences in the selected data are seasonally dependent because of the liberal angular and time allowances used here to match the data. That is, the average

differences in time and, therefore, solar zenith angle, viewing zenith angle, or relative azimuth angle between the two satellites may systematically vary with season, with the sign of a given difference flipping at some point as the inter-satellite configuration changes over the year. Using the annual average should account for those seasonal changes and should be unbiased on the whole. Doelling et al. [22] applied much tighter restrictions for matching Terra and Aqua to compute slopes for each month between 2002 and 2012. Their results show no seasonal cycles similar to those observed here, indicating that the angular configurations are the likely culprit for the apparent seasonal changes in gain.

The datasets in Fig. 3a are closest during the initial period, although the C5' results tend to have the greatest values. The slopes are separated by 2008 (days 2050-2466), although the C5' and C6 differences are relatively close. Slope and difference separations are greatest around day 4000 when the C5 values are markedly less than their C5' and C6 counterparts. The C5' and C6 results remain fairly close during the last 2 years.

To put the results on a roughly equivalent radiance basis (Earth-Sun distance variations are neglected), the reflectances were multiplied by the  $\cos(\text{SZA})$ . The slope behavior (Fig. 3b) is a bit cleaner than the unnormalized results, but remains essentially the same as the unnormalized data. The magnitude of the differences in the normalized reflectances decreases significantly and the separation of the C5 values from the others is a little clearer. Despite the variability during the year, it is evident that the Terra C5' and C6 reflectances are relatively close, particularly during the latter years, and exceed their the C5 reflectances, which are consistently less than their Aqua counterparts.

This behavior is seen more clearly in the annual means. These are shown in Fig. 4 for channels 1, 5, 7, and 26 using the SZA-normalized reflectances. The C5 and C6 0.63- $\mu\text{m}$  slopes (Fig. 4a) and differences (Fig. 4b) are nearly equal during 2003 and diverge afterwards, with the C6 means remaining fairly constant between 0.97 and 0.98 over the 15 years. The mean differences (Fig. 4b) mimic the slopes. The C5' differences are near zero during 2003, 2008, and 2016, but drop to almost -0.002, below the C6 mean, in 2013. The C5 minimum difference of almost -0.008 also occurs during 2013. The C6 differences average out to approximately -0.002 with a maximum in 2013.

The interannual variability in channel 5 is less dramatic than for channel 1. The slopes (Fig. 4c) for C5 and C6 are very similar,  $\sim 1.005$ , except during the last 2 years when the C6 values dip below the C5 slopes. The C5' slope is fairly steady around 0.98. The original Terra C5 calibration produces mean normalized reflectance differences of  $\sim -0.006$  relative to Aqua C5 (Fig. 4d), a value similar to the C6 differences before 2014. A change in the Terra-Aqua relationship must have occurred between 2013 and 2015, as the C6 differences dropped to 0.004, while the C5' values rose from near zero to 0.002.

Channel 26 is somewhat like channel 5 in that it appears that few changes were made to the Terra calibration between C5 and C6, as their slopes (Fig. 4e) and differences (Fig. 4f) relative to the matched Aqua data are very close throughout the study period. The differences drop from -0.0003 to almost

-0.0005, while the slopes decrease by  $\sim 0.04$ . The C5' slopes and differences drop by almost 0.03 and from -0.00012 to -0.00025 during the same time. While these values seem quite small, the mean reflectance for channel 26 is  $\sim 0.01$ , so a 0.0002 difference is a 2% bias. Because channel 26 is so sensitive to water vapor absorption by very narrow lines, small differences in the SRFs could produce significant differences in reflectance. The impact of the SRFs on the Terra-Aqua relationships were estimated from calculations performed using the spectral integration computational system of [24] for spectral data over the polar regions. It was found that, except for channel 26, the SRF differences produce ratios of 0.999-1.003. For the 1.38- $\mu\text{m}$  channel, however, the SRF differences yield a correction of 1.014, a value roughly one third that in Table II. Thus, the correction used for Ed4 may overadjust the Terra reflectances by a third too much. Nevertheless, the correction should improve the Aqua-Terra channel-26 consistency relative to that from C5 and C6 data.

At 2.13  $\mu\text{m}$ , the C5 and C6 slopes (Fig. 4g) and differences (Fig. 4h) are again very similar, but not as close as for 1.38  $\mu\text{m}$ . In this case, the adjustments to C5, seen in the C5' results, appear to have diminished the consistency of the Terra and Aqua channels between 2008 and 2015 and possibly for some years prior to 2008 as the slopes are the smallest and the magnitudes of differences greatest for those periods. Relative to the mean reflectance, the C5' differences convert to approximately -1%. For this band, the Terra C6 calibration appears to be most consistent with Aqua with a mean difference near zero.

For the evaluations in Figs. 3 and 4, is the annual average difference a reliable reference? Here again, the results of [22] provide reference points for comparison of the results. In their Table IV, Doelling et al. [22] listed the normalization slopes and their trends and means for the period 2002-2012. Their average values for both nadir matches and off-nadir matches are reproduced in Table II along with the averages computed for the same time period using the coefficients in Table I. The mean Ed4 values for channels 1, 4, 5, 7, and 27 are all within  $\pm 0.2\%$  of the presumably more accurate, previously published values. For channels 2 and 3, the Ed4 coefficients underestimate gain change by 0.6 and 1.0%, respectively. Fortunately for the Ed4 cloud retrievals, those two channels have minimal influence on the results. In general, therefore, there should be minimal differences between the Terra and Aqua products due to intercalibration discrepancies in the solar channels, at least, through 2012. This is what the mean differences in Fig. 4 show. The C5'-C6 annual mean differences are all quite close to zero. The mean slopes, however, are not as close to the predicted values (Table I) as would be expected. Slopes, being ratios for forced fits, are not linearly related and would not be expected to produce the correct result through linear averaging. Thus, the mean difference is a more reliable metric for the evaluation.

### B. Shortwave Infrared Channel

The changes in the Terra C5 SIR channel calibration also result in much greater consistency between Terra and Aqua. Fig. 5 shows comparisons of matched Terra and Aqua Channel-20 brightness temperature data for day (top) and night (bottom), 11 April 2015. During the day, the original C5

temperatures (Fig. 5a) differ by  $\sim 0.5$  K, a value close to that reported by [13]. The C6 data (Fig. 5b) yield a smaller difference,  $T_{Te} - T_{Aq}$ , of 0.1 K suggesting that the Terra calibration changed for C6 over the observed range. The CERES adjustment applied to the C5 data during the daytime (Fig. 5c) also reduces  $|T_{Te} - T_{Aq}|$  to less than 0.1 K. At night, the Terra C5 temperatures (Fig. 5d) asymptote at  $\sim 220$  K, while  $T_{Aq}$  drops to values as low as 200 K, as seen earlier. The mean difference is 2.1 K. The C6 calibrations (Fig. 5e) straighten the curve, resulting in much better agreement, a difference of 0.2 K, between Aqua and Terra at the low temperatures. Applying the CERES corrections to  $T_{Te}$  (Fig. 5f) also results in excellent agreement with a 0.0 K mean differences. The C6 and C5' standard deviations are less than their C5 counterpart.

These results are fairly typical. Fig. 6 plots the daily and monthly mean temperature differences between Terra collections C5, C5', and C6 and their Aqua C6 counterparts. The daytime daily differences (Fig. 6a) for all Terra versions have distinct seasonal variations, ranging over  $\sim 2$  K. The peak occurs around February and the minimum around November. The C5-C5 nocturnal differences (Fig. 6c) have a distinct variation of  $\sim 1.5$  K each year with minima in January and December with a peak near the boreal summer solstice. For the C6-C6 and C5'-C6 values, the seasonal cycles are reduced to  $\sim 0.3$  K and have a slightly different phasing. Since the  $3.8\text{-}\mu\text{m}$  channel has a solar reflected component, it follows the same seasonal pattern as the visible channel during the daytime (Fig. 3). The nighttime seasonal variation in the C5-C5 differences is due to disparity in the relative frequency of very low temperatures observed over the Arctic and Antarctic, the latter being colder, on average.

The trends are clearer in the annual means. The average daytime (Fig. 6b) C5 Terra-Aqua difference decreases from 0.65 K in 2003 to 0.45 K in 2016, while the C6-C6 and C5'-C6 differences drop from 0.27 K to 0.12 K and from 0.06 K to -0.16 K, respectively. At night (Fig. 6d), the C5-C5 differences hover around 2.0 K. The C6 and C5' Terra mean temperatures differ from their Aqua counterparts by roughly 0.2 K and 0.0 K, respectively. No trend is evident in the nighttime differences.

### C. Longwave Infrared Channels

Although no changes were applied to the longer wavelength channels, it is instructive to examine the inter-satellite consistency of the relevant channels to understand their potential impact on any retrievals. The monthly comparisons between Terra and Aqua MODIS channels were performed for the period 2002- 2016. The results are summarized here using daytime and nighttime data together.

1) *Channels 27 and 29*: The primary water vapor band, channel 27, showed some changes over time as reported by [25] and shown in Figs. 7 and 8 for nighttime and daytime data, respectively. At night, the Aqua and Terra  $6.78\text{-}\mu\text{m}$  temperatures were very close on 11 July 2003 in both the C5 (Fig. 7a) and C6 (Fig. 7d) data, but by 11 July 2008, the Terra C5 temperatures (Fig. 7b) were slightly less than their Aqua counterparts at the low end resulting in a mean temperature differences of 0.55 K. By 11 July 2015 (Fig. 7c), the difference at the low end increased, resulting in a bias of 0.8

K. The C6 adjustments appear to have corrected the low-end bias but decreased the upper end resulting in average Terra-Aqua differences of -1.3 and -2.9 K by 11 July 2008 and 2015, respectively. The forced linear fits dropped from 0.987 in 2003 to 0.928 in 2015. During daytime, when matched data were taken mostly in the northern polar regions, the lowest end of the range is not represented and the differences are no longer positive, on average. On 11 July 2003, the daytime C5 and C6 mean biases are -0.2 and -0.7 K (not shown), respectively. By 2015, the differences are strongly negative for both C5 (Fig. 8a) and C6 (Fig. 8b). Combining the day and night data tends to favor the upper end of the scale.

The trends in the channel-27 Terra-Aqua differences are more evident in the time series of monthly mean differences plotted in Fig. 9 for combined day and night matched data. The average C5 difference (Fig. 9a), which reflects the degree of low-end divergence, begins slightly positive and gradually falls below zero to around -1 K by 2015. During 2016, the differences drop suddenly in mid-February and do not recover, as first reported by Wilson et al. (2017). The C6 trend (Fig. 9b) is much steeper, beginning with a small negative value and reaching nearly 4 K in mid-2015. Apparently the C6 revision of the  $6.78\text{-}\mu\text{m}$  channel corrected the low-end bias (Fig. 7) with the effect of causing a bias at higher temperatures. The drop during February 2016 is much more evident in the C6 data and suggests that Terra channel-27 data taken after the plunge should not be used as they are poorly correlated and have significant inter-detector striping (not shown).

Fig. 10 presents scatter plots and fits for the same Terra-Aqua matches seen in Fig. 7, except that the channel-29 ( $8.55\text{-}\mu\text{m}$ ) data are used. The C5 data are well correlated linearly in 2003 (Fig. 10a) with mean difference of 0.4 K. The linear structure gives way over time to positive biases in Terra at the low end of the range resulting in average differences of 0.9 K in 2008 (Fig. 10b) and 3.2 K in 2015 (Fig. 10c) for these 11 July matches. Calibration adjustments used for the C6 collection appear to have eliminated most or all of the differences through 2015 as the linear structure is retained in Figs. 10d-f and the magnitude of the mean differences is 0.2 K or less in these examples. The monthly mean Terra-Aqua differences in Fig. 11 are near zero before 2008 and then rise to values greater than 3 K by late 2015 (Fig. 11a). The linear fit of the trend produces a slope that is 3x that of the fit to the C6 data (Fig. 11b). For the latter, the mean difference starts as a small negative value that becomes positive over time and bumps up by  $\sim 0.5$  K in 2016 to 1 K.

2) *Channels 31, 32, 33*: For Collection 5, the mean difference between Terra and Aqua for the entire period at  $10.8\text{-}\mu\text{m}$  (channel 31) is 0.05 K. For the  $12.0$  and  $13.4\text{-}\mu\text{m}$  channels, the average differences are 0.02 K and -0.05 K, respectively. No significant trend in the differences was found for any of the three channels. The Collection 6 consistency is similar. For channels 31, 32 ( $12.0\text{-}\mu\text{m}$ ), and 33 ( $13.4\text{-}\mu\text{m}$ ), the Terra-Aqua differences are -0.07, -0.09, and -0.12 K, respectively. Again, no trends in the differences were observed. The fitted linear slopes typically differed from 1.000 by less than  $\pm 1\%$  for both collections, indicating that the consistency between Terra and Aqua occurred at all values.

#### IV. CALIBRATION IMPACT ON RETRIEVED CLOUD PROPERTIES

The above comparisons indicate that when corrections were applied to the C5 data for CERES Ed4, they generally resulted in Terra-Aqua consistency that was as good as or better than that of the C6 datasets. When corrections were neither developed nor applied, some artifacts are likely to be introduced into the Ed4 cloud property record. For example, the solar channel corrections were developed using the Aqua data and were only applied during the Aqua period. The pre-Aqua period for Terra could produce an anomaly because of the absent corrections. These and other aspects of the Terra and Aqua calibrations are discussed below. While it is beyond the scope of this paper to illustrate the impact of the calibration changes on all of the various cloud properties, a few examples are given to highlight the importance of the corrections. The cloud properties presented here are available from the CERES Ed4 SSF, and SSF1deg-hour, -day and -month single satellite data products.

##### A. Solar Channels

Since channel 1 is the primary solar channel used for cloud detection and optical depth retrieval over non-snow surfaces in both Ed2 and Ed4 algorithms [13, 17, 19, 26] the calibration of this channel has significant influence on the cloud retrievals. Likewise, over snow, the 1.24- $\mu\text{m}$  channel is the primary channel for optical depth retrieval. Fig. 12 plots the trends in Terra and Aqua cloud optical depths (COD) for Ed2 based on C5 data and Ed4 based on C5' data for both non-polar (60°S – 60°N latitudes) and polar (poleward of 60° latitude) regions. The mean non-polar (Fig. 12a) Terra Ed2 CODs (shown in gold) are relatively flat in the initial years and have a downward trend after 2003 (Fig. 12a), dropping by more than 10% between 2003 and 2012. The trend is not continuous, but tends to reflect the discontinuities assumed in Table I. The Aqua Ed2 CODs (shown in aqua blue) are between 4 and 9% greater than their Terra counterparts and have a slower downward trend of -4.1%/decade. Using the C5' calibration for Terra brings the Ed4 COD means for the two instruments into much better agreement. Although there is no particular reason for Terra (shown in red) and Aqua (shown in blue) to have the same average optical depths, they are taken 3 hours apart, they would likely have similar trends if their calibrations are consistent. During the pre-Aqua period, the Ed4 Terra COD is up to 4% less than its value at the beginning of the Aqua period. The pre-Aqua differences between the Terra Ed2 and Ed4 CODs are primarily due to the changes in cloud fraction between Ed2 and Ed4. More optically thin clouds were detected in Ed4 than in Ed2, reducing the average optical depth. This effect is also seen the Aqua COD averages, especially in the early years. From the sharp rise in Terra Ed4 COD before the Aqua period, it is clear that the C5' 1% channel-1 calibration adjustment (Table I) should have been extended back to the time of the Terra launch.

Despite the inter-satellite consistency in the Ed4 results, the Aqua CODs still have a trend of -3.3%/dec. The Terra Ed4 trend is similar to that for Aqua, if only data after 2002 are considered. This decrease in COD over time is most likely due to degradation in the Aqua channel-1 calibration seen after 2007. Doelling et al. [22] showed that the Aqua C6 gain

dropped by 1%/dec. Because there were only minor changes between Aqua C5 and C6, the Aqua C5 gain had the same trend. This degradation was not discovered prior to Ed4 processing and was not included in the C5' calibrations. Since the Terra C5' calibration depends on Aqua, the Terra Ed4 CODs decrease at the same rate as the Aqua means as long as other changes do not occur in the Terra calibrations after 2009.

Over the polar regions (Fig. 12b), the Ed2 CODs differ by ~20%. The Terra Ed2 means have a slightly decreasing trend, while their Aqua counterparts remain relatively constant. For Ed2, the 1.6 and 2.1- $\mu\text{m}$  channels were used to retrieve cloud optical depth over snow. Thus, the differences in the CODs are not surprising as the 2.1- $\mu\text{m}$  reflectance saturates at a lower COD than the 1.6- $\mu\text{m}$  reflectance. In the Ed4 processing, the 1.24- $\mu\text{m}$  channel was used over snow to retrieve COD for both satellites. The resulting mean Terra and Aqua CODs differ by ~5% and the Terra averages have a negative trend during the Aqua period that is steeper than the -0.16/dec trend in Aqua COD. This suggests that the calibration correction after 2003 should have been larger. The absence of a correction prior to the Aqua launch is evident in the 10% drop in the Terra Ed4 mean COD from 2001 to 2003. The Terra Ed4 results in Fig. 12 suggest that there may be some changes in Terra after 2014 that were not included in Table I. It is likely, therefore, that the greater C5'-C5 differences in Fig. 12 after 2012 are due to adjustments to Terra.

From the examples in Fig. 12, it is clear that reflectance calibration corrections have significant impacts on the retrievals and can either improve or decrease the consistency and accuracy of the results. Impacts due to changes in other solar channels are left for future papers.

##### B. Shortwave Infrared

Overall, the change in the SIR calibration will tend to affect the Terra cloud particle effective radius, CER, during the day. As seen in Fig. 13a, the mean Ed2 nonpolar liquid CER from Terra is 0.3 to 0.4- $\mu\text{m}$  smaller than its Aqua counterpart. For Ed4, the Terra and Aqua CERs differ by less than 0.1  $\mu\text{m}$ . The Terra Ed2 CER for ice clouds is nearly 2- $\mu\text{m}$  greater than the Aqua mean (Fig. 13b), but the Ed4 ice CERs are in excellent agreement for nonpolar areas. The increase in the Aqua ice CER from Ed2 to Ed4 is due to the use of a new ice crystal model in the retrieval and some changes in the cloud population. The main point is that the same algorithm is applied to both satellite datasets and the Ed4 CER values agree much better than the corresponding Ed2 values. Trends of -0.8 and -0.5 %/dec in the Ed4 Terra and Aqua ice CER means are greater than the corresponding -0.5 and -0.2 %/dec for liquid cloud values. Since the CER retrieval depends to some extent on the COD, these trends may simply be the result of the COD trends seen in Fig. 12.

The SIR channel is also used along with many others in the cloud mask and cloud phase selection algorithms. Thus, the impact of the SIR calibration on those other parameters is more complicated than seen for the CER retrieval. These other effects of adjusting the Terra SIR calibration will be discussed in future reporting.

##### C. Infrared Channels

The lack of adjustments to the 6.7 and 8.5- $\mu\text{m}$  data also has

significant impacts on the CERES Ed4 properties. For example, the 8.5- $\mu\text{m}$  channel is used in the Ed4 phase selection [19], particularly at night. Fig. 14 plots the 12-month running mean, non-polar proportions of liquid and ice clouds at night. The Terra and Aqua Ed2 mean liquid cloud fractions track each other well and show very little trending. Since the Ed2 phase selection does not employ the 8.5- $\mu\text{m}$  channel, it is unaffected by any of its calibration artifacts. On the other hand, the Ed4 Terra liquid fraction appears to decrease slowly between 2000 and 2012, then drops at a much steeper rate through 2016. Meanwhile, the Ed4 Aqua liquid fraction is relatively steady throughout the record with a trend of 0.005/dec. Comparing with the difference trend in Fig. 9a (the differences trend for 8.5- $\mu\text{m}$  is similar to that for 6.7- $\mu\text{m}$  (not shown)), it is clear that the 8.5- $\mu\text{m}$  channel calibration is the primary cause for the nocturnal phase trend in the Terra Ed4 liquid cloud fraction. This result is not surprising since the 8.5- $\mu\text{m}$  phase selection criteria are based on small brightness temperature differences. Even a tiny calibration trend in one of the two differencing channels calibration is sufficient to bias the results using those brightness temperature differences.

## V. CONCLUSIONS

Calibration adjustments were developed and applied to certain Terra C5 channels to account for known differences in Terra C5 and its Aqua MODIS C5 counterparts in order to achieve inter-satellite consistency in the CERES Ed4 cloud property retrievals. The main Terra-MODIS findings are summarized for each channel as follows.

- 1) Channel 1 (0.64  $\mu\text{m}$ ): Between July 2002 and 2016, the magnitude of the annual mean Terra-Aqua (T-A) reflectance difference after correction is less than 0.002 with an average of less than 0.001. The Terra correction was not applied prior to the Aqua period and does not account for a 1%/dec degradation in the Aqua gain after 2008. That degradation remains in the Aqua C6 data [22]. The Terra C6 reflectances, however, appear to be trendless differ from their Aqua counterparts by an average of -0.002 over the record.
- 2) Channel 5 (1.24  $\mu\text{m}$ ): The T-A reflectance differences for the corrected C5 data after July 2002 are similar to the channel-1 results. No correction was applied to the Terra C5 data before July 2002. A significant T-A bias of 0.006 is present in both the Terra C6 and uncorrected C5 data.
- 3) Channel 7 (2.13  $\mu\text{m}$ ): The correction applied to the C5 Terra data increased the magnitude of the T-A difference by a factor of 2. The C6 Terra data are more consistent with Aqua C5 than either version of the C5 data.
- 4) Channel 20 (3.78  $\mu\text{m}$ ): Biases in the T-A brightness temperature differences have been effectively removed in the corrected Terra C5 data for both day and night. Small T-A biases of  $\sim 0.2\text{K}$  remain in both day and night Terra C6 data.
- 5) Channel 26 (1.38  $\mu\text{m}$ ): The mean T-A reflectance difference for the corrected data is very small, but still equivalent to -1%. For Terra C6, the difference averages to -3%.
- 6) Channel 27 (6.71  $\mu\text{m}$ ): No corrections were applied to the

Terra C5 data, but T-A differences at the low end of the temperature range slowly developed and became significant after 2011 in the C5 data. The Terra C6 data show a significant downward trend in T-A beginning in 2002. A large drop in both the Terra C5 and C6 Terra temperatures occurred in 2016.

- 7) Channel 29 (8.55  $\mu\text{m}$ ): The Terra C5 data were not corrected and suffered from a gradually increasing T-A temperature difference from 2002 onward. This trend is mostly eliminated in the C6 data.
- 8) Channels 31, 32, and 33 (11.0, 12.0, and 13.3  $\mu\text{m}$ ): No corrections were applied to these channels for C5 data. The C5 T-A differences, having a magnitude of 0.1 K or less, are expected to have minimal impact on the consistency between the Terra and Aqua cloud properties.

All corrections assumed that the relationship between each pair of channels is constant throughout the record and that neither the Aqua nor the Terra MODIS channel calibrations changed after 2009. Analyses in this paper determined that for the channels that were altered, the corrections successfully achieved the desired consistency in both the radiances and Ed4 cloud properties, except when the latter stability assumption was violated. In general, the agreement between the Aqua C5 and adjusted Terra C5 radiances is generally equivalent to or better than that found for their C6 counterparts.

Despite the consistency achieved for the Terra and Aqua datasets in Ed4, the CERES Ed4 SSF based cloud property datasets should be used cautiously for cloud trend studies. The remaining calibration differences noted above have produced some significant artifacts in the cloud properties that affect their use for studying long-term trends in the cloud properties and cloud-radiation interactions. To eliminate those artifacts, it is clear that further adjustments are needed in the MODIS C6 calibrations before reprocessing the CERES cloud properties. Wilson et al. [25] recently identified and addressed the problems in the C6 data discussed here for channels 27 and 29. Likewise, Angal et al. [27] found the cause of the drift in the Aqua calibration for channels 1-4 and found corrections for it. Those corrections and the adjustments of [25] have been incorporated into a new MODIS Level-1B radiance dataset, Collection 6.1, that is being processed as of this writing [28]. Using that new MODIS collection along with the adjustments to Terra channels 5 and 26 discussed here to reprocess the CERES cloud properties should eliminate the artifacts in the cloud property record noted here and elsewhere. The following list outlines the different types of graphics published in IEEE journals. They are categorized based on their construction, and use of color / shades of gray:

## REFERENCES

- [1] B. A. Wielicki, B. R. Barkstrom, B. A. Baum, T. P. Charlock, R. N. Green, D. P. Kratz, R. B. Lee, P. Minnis, G. L. Smith, D. F. Young, R. D. Cess, J. A. Coakley, D. A. H. Crommelynck, L. Donner, R. Kandel, M. D. King, A. J. Miller, V. Ramanathan, D. A. Randall, L. L. Stowe, and R. M. Welch, "Clouds and the Earth's Radiant Energy System (CERES): Algorithm Overview," *IEEE Trans. Geosci. Rem. Sens.*, vol. 36, pp. 1127-1141, 1998.
- [2] C. Stubenrauch, W. B. Rossow, S. Kinne, S. Ackerman, G. Cesana, H. Chepfer, B. Getzewich, L. DiGirolamo, A. Guignard, A. Heidinger, B. Maddux, P. Menzel, P. Minnis, C. Pearl, S. Platnick, C. Poulsen, J.

- Riedi, S. Sun-Mack, A. Walther, D. Winker, S. Zeng, and G. Zhao, "Assessment of global cloud datasets from satellites: Project and database initiated by the GEWEX Radiation Panel," *Bull. Am. Meteorol. Soc.*, vol. 94, pp. 1031-1049, doi:10.1175/BAMS-D-12-00117, 2013.
- [3] M. J. Foster, S. A. Ackerman, K. Bedka, R. A. Frey, L. DiGirolamo, A. K. Heidinger, S. Sun-Mack, B. C. Maddux, W. P. Menzel, P. Minnis, M. Stengel, and G. Zhao, "Cloudiness [in "State of the Climate 2015"]," *Bull. Amer. Meteorol. Soc.*, vol. 97, pp. S28-S29, 2016.
- [4] M. J. Foster, S. A. Ackerman, R. A. Frey, L. DiGirolamo, A. K. Heidinger, S. Sun-Mack, W. P. Menzel, P. Minnis, G. Zhao, "Cloudiness [in "State of the Climate 2016"]," *Bull. Amer. Meteorol. Soc.*, vol. 98, pp. S27-S28, 2017.
- [5] M. H. Zhang, W. Y. Lin, S. A. Klein, J. T. Bacmeister, S. Bony, R. T. Cederwall, A. D. Del Genio, J. J. Hack, N. G. Loeb, U. Lohmann, P. Minnis, I. Musat, R. Pincus, P. Stier, M. J. Suarez, M. J. Webb, J. B. Wu, S. C. Xie, M.-S. Yao, and J. H. Zhang, "Comparing clouds and their seasonal variations in 10 atmospheric general circulation models with satellite measurements," *J. Geophys. Res.*, vol. 110, doi: 10.1029/2004JD005021, 2005.
- [6] D. Waliser, F. Li, C. Woods, R. Austin, J. Bacmeister, J. Chern, A. DelGenio, J. Jiang, Z. Kuang, H. Meng, P. Minnis, S. Platnick, W. B. Rossow, G. Stephens, S. Sun-Mack, W. K. Tao, A. Tompkins, D. Vane, C. Walker, and D. Wu, "Cloud ice: A climate model challenge with signs and expectations of progress," *J. Geophys. Res.*, vol. 114, D00A21, doi:10.1029/2008JD010015, 2009.
- [7] R. E. Stanfield, X. Dong, B. Xi, A. D. Del Genio, P. Minnis, and J. Jiang, "Assessment of NASA GISS CMIP5 and post-CMIP5 simulated clouds and TOA radiation budgets using satellite observations. Part I: Cloud fraction and properties," *J. Climate*, vol. 27, pp. 4189-4208, doi: 10.1175/JCLI-D-13-00558.1, 2014.
- [8] X. Xiong, K. Chiang, A. Wu, W. Barnes, B. Guenther, and V. Salomonson, "Multiyear on-orbit calibration and performance of Terra MODIS thermal emissive bands," *IEEE Trans. Geosci. Remote Sens.*, vol. 46, pp. 1790-1803, 2008.
- [9] X. Xiong, J. Sun, W. Barnes, V. Salomonson, J. Esposito, H. Erives, and B. Guenther, "Multiyear on-orbit calibration and performance of Terra MODIS reflective solar bands," *IEEE Trans. Geosci. Remote Sens.*, vol. 45, pp. 879-889, 2007.
- [10] X. Xiong, J. Sun, X. Xie, W. L. Barnes, and V. V. Salomonson, "On-orbit calibration and performance of Aqua MODIS reflective solar bands," *IEEE Trans. Geosci. Remote Sens.*, vol. 48, pp. 535-546, doi:10.1109/TGRS.2009.2024307, 2010.
- [11] X. Xiong, B. Wenny, A. Wu, W. L. Barnes, and V. Salomonson, "Aqua MODIS thermal emissive bands on-orbit calibration, characterization, and performance," *IEEE Trans. Geosci. Remote Sens.*, vol. 47, pp. 803-814, 2009.
- [12] P. Minnis, D. R. Doelling, L. Nguyen, W. F. Miller, and V. Chakrapani, "Assessment of the visible channel calibrations of the TRMM VIRS and MODIS on Aqua and Terra," *J. Atmos. Oceanic Technol.*, vol. 25, pp. 385-400, 2008.
- [13] P. Minnis, Q. Z. Trepte, S. Sun-Mack, Y. Chen, D. R. Doelling, D. F. Young, D. A. Spangenberg, W. F. Miller, B. A. Wielicki, R. R. Brown, S. C. Gibson, and E. B. Geier, "Cloud detection in non-polar regions for CERES using TRMM VIRS and Terra and Aqua MODIS data," *IEEE Trans. Geosci. Remote Sens.*, vol. 46, pp. 3857-3884, 2008.
- [14] B. N. Wenny, J. Sun, X. Xiong, A. Wu, H. Chen, A. Angal, T. Choi, N. Chen, S. Madhavan, X. Geng, J. Kuyper, and L. Tan, "MODIS calibration algorithm improvements developed for Collection 6 Level-1B," *Earth Observing Systems XI, Proc. SPIE*, vol. 7807, 78071F-9, doi:10.1117/12.860892, 2010.
- [15] X. Dong, P. Minnis, B. Xi, S. Sun-Mack, and Y. Chen, "Comparison of CERES-MODIS stratus cloud properties with ground-based measurements at the DOE ARM Southern Great Plains site," *J. Geophys. Res.*, vol. 113, D03204, 17 pp. doi:10.1029/2007JD008438, 2008.
- [16] P. Minnis, S. Sun-Mack, Y. Chen, M. M. Khaiyer, Y. Yi, J. K. Ayers, R. R. Brown, X. Dong, S. C. Gibson, P. W. Heck, B. Lin, M. L. Nordeen, L. Nguyen, R. Palikonda, W. L. Smith, Jr., D. A. Spangenberg, Q. Z. Trepte, and B. Xi, "CERES Edition-2 cloud property retrievals using TRMM VIRS and Terra and Aqua MODIS data, Part II: Examples of average results and comparisons with other data," *IEEE Trans. Geosci. Remote Sens.*, vol. 49, no. 11, pp. 4401-4430, doi:10.1109/TGRS.2011.2144602, 2011.
- [17] P. Minnis, S. Sun-Mack, D. F. Young, P. W. Heck, D. P. Garber, Y. Chen, D. A. Spangenberg, R. F. Arduini, Q. Z. Trepte, W. L. Smith, Jr., J. K. Ayers, S. C. Gibson, W. F. Miller, V. Chakrapani, Y. Takano, K.-N. Liou, Y. Xie, and P. Yang, "CERES Edition-2 cloud property retrievals using TRMM VIRS and Terra and Aqua MODIS data, Part I: Algorithms," *IEEE Trans. Geosci. Remote Sens.*, vol. 49, no. 11, pp. 4374-4400, doi:10.1109/TGRS.2011.2144601, 2011.
- [18] G. Toller, X. Xiong, J. Sun, B. N. Wenny, X. Geng, J. Kuyper, A. Angal, H. Chen, S. Madhavan, and A. Wu, "Terra and Aqua moderate resolution imaging spectroradiometer collection 6 level 1B algorithm," *J. Appl. Remote Sens.*, vol. 7, 073557, doi: 10.1117/1.JRS.7.073557, 2013.
- [19] P. Minnis, S. Sun-Mack, Q. Z. Trepte, F.-L. Chang, P. W. Heck, Y. Chen, Y. Yi, R. F. Arduini, K. Ayers, K. Bedka, S. Bedka, R. Brown, S. Gibson, E. Heckert, G. Hong, Z. Jin, R. Palikonda, R. Smith, W. L. Smith, Jr., D. A. Spangenberg, P. Yang, C. R. Yost, and Y. Xie, "CERES Edition 3 cloud retrievals," *Proc. AMS 13<sup>th</sup> Conf. Atmos. Rad.*, Portland, OR, 5.4, 7 pp., June 27-July 2, 2010. (<https://ams.confex.com/ams/13CldPhy13AtRad/webprogram/Paper171366.html>)
- [20] A. Wu, X. Xiong, D. R. Doelling, D. Morstead, A. Angal, and R. Bhatt, "Characterization of Terra and Aqua MODIS VIS, NIR, and SNIR spectral and calibration stability," *IEEE Trans. Geosci. Remote Sens.*, vol. 51, pp. 4330-4338, doi:10.1109/TGRS.2012.226588, 2013.
- [21] X. Xiong, A. Angal, J. Butler, C. Cao, D. Doelling, A. Wu, and X. Wu, "Global Space-Based Inter-Calibration System reflective solar calibration reference: From Aqua to S-NPP VIIRS," *Proc. SPIE Earth Observing Missions and Sensors: Development, Implementation, and Characterization IV*, vol. 9881, no. 98811D, 12 pp., 2016.
- [22] D. R. Doelling, A. Wu, X. Xiong, B. R. Scarino, R. Bhatt, C. O. Haney, D. Morstad, and A. Gopalan, "The radiometric stability and scaling of Collection 6 Terra- and Aqua-MODIS VIS, NIR, and SWIR spectral bands," *IEEE Trans. Geosci. Remote Sens.*, vol. 53, pp. 4520-4535, doi:10.1109/TGRS.2015.2400928, 2015.
- [23] Li, Y., A. Wu, and X. Xiong, "Evaluating calibration of MODIS thermal emissive bands using infrared atmospheric sounding interferometer measurements," *Proc. SPIE 8724, Ocean Sensing and Monitoring V*, vol. 87240X, doi:10.1117/12.2016621, June, 2013.
- [24] B. R. Scarino, D. R. Doelling, P. Minnis, A. Gopalan, T. Chee, R. Bhatt, C. Lukashin, and C. O. Haney, "A web-based tool for calculating spectral band difference adjustment factors derived from SCIAMACHY hyperspectral data," *IEEE Trans. Geosci. Remote Sens.*, vol. 54, no. 5, pp. 2529-2542, 2016.
- [25] T. Wilson, A. Wu, A. Shrestha, X. Geng, Z. Wang, C. Moeller, R. Frey, and X. Xiong, "Development and Implementation of an Electronic Crosstalk Correction for Bands 27-30 in Terra MODIS Collection 6," *Remote Sens.*, vol. 9, 21 pp., doi:10.3390/rs9060569, 2017.
- [26] Q. Z. Trepte, P. Minnis, C. R. Trepte, S. Sun-Mack, and R. Brown, "Improved cloud detection in CERES Edition 3 algorithm and comparison with the CALIPSO Vertical Feature Mask," *Proc. AMS 13<sup>th</sup> Conf. Atmos. Rad. and Cloud Phys.*, Portland, OR, no. JP1.32, June 27 - July 2, 2010. (<https://ams.confex.com/ams/13CldPhy13AtRad/webprogram/Paper171785.html>)
- [27] A. Angal, X. Xiong, A. Wu, X. Geng, and H. Chen, "Improvements in the on-orbit response versus scan angle characterization of the Aqua MODIS reflective solar bands," *IEEE Trans. Geosci. and Remote Sensing*, submitted, 2017.
- [28] MODIS Characterization Support Team, "Level-1B (L1B) calibration, Collection 6.0 and Collection 6.1 changes," *MODIS Data Alert*, 21 October, 9 pp. Available at ([https://modis-atmosphere.gsfc.nasa.gov/sites/default/files/ModAtmo/C061\\_L1B\\_Combined\\_v8.pdf](https://modis-atmosphere.gsfc.nasa.gov/sites/default/files/ModAtmo/C061_L1B_Combined_v8.pdf)), 2017.





TABLE I  
 CALIBRATION COEFFICIENTS FOR (2) FOR TERRA MODIS COLLECTION 5 ED4 REFLECTANCES/RADIANCES

Channel	14 May 2002 -18 Nov 2003		19 Nov 2003 – 31 March 2009		After 31 March 2009	
	a <sub>0</sub>	a <sub>1</sub>	a <sub>0</sub>	a <sub>1</sub>	a <sub>0</sub>	a <sub>1</sub>
1 (0.65 μm)	1.0100	0.0	1.0190	0.0	1.0320	0.0
2 (0.87 μm)	0.9996	0.0	1.0010	2.904 x 10 <sup>-6</sup>	1.0059	0.0
3 (0.47 μm)	0.9958	1.182 x 10 <sup>-5</sup>	0.9997	9.662 x 10 <sup>-6</sup>	1.0368	0.0
4 (0.55 μm)	1.0016	0.0	1.0105	0.0	1.0219	0.0
5 (1.24 μm)	0.9724	0.0	0.9736	0.0	0.9706	0.0
7 (2.13 μm)	0.9927	0.0	0.9957	0.0	0.9995	0.0
26 (1.38 μm)	1.0307	0.0	1.0429	0.0	1.0430	0.0

TABLE II  
MEAN CALIBRATION COEFFICIENTS FOR TERRA MODIS COLLECTION 5, JUNE 2002-DECEMBER 2012

Channel	Doelling et al. [22] nadir (off)	CERES Ed4 Clouds
1 (0.65 $\mu\text{m}$ )	1.021 (1.021)	1.022
2 (0.87 $\mu\text{m}$ )	1.008 (1.007)	1.002
3 (0.47 $\mu\text{m}$ )	1.023 (1.018)	1.011
4 (0.55 $\mu\text{m}$ )	1.012 (1.012)	1.013
5 (1.24 $\mu\text{m}$ )	0.970 (0.971)	0.972
7 (2.13 $\mu\text{m}$ )	0.999 (0.999)	0.997
26 (1.38 $\mu\text{m}$ )	1.041 (1.039)	1.041

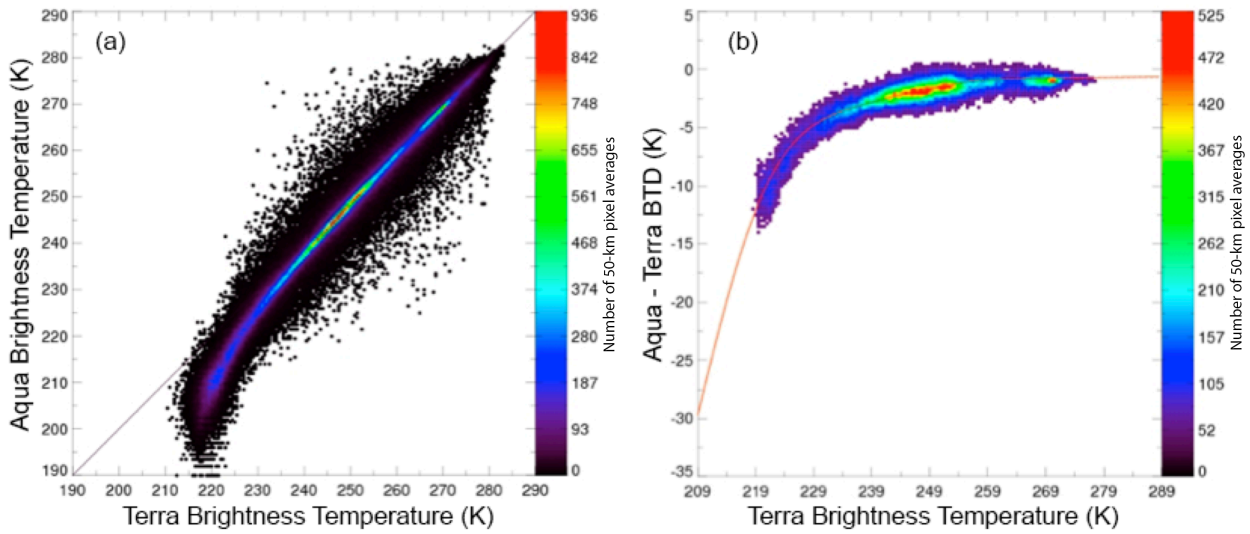


Fig. 1. Scatterplots of (a) Aqua and Terra SIR temperatures for July 2007, and (b) the corresponding SIR temperature difference between Aqua and Terra as a function of Terra SIR temperatures. Red line is Terra 3.8- $\mu$ m night time calibration curve for July 2007.

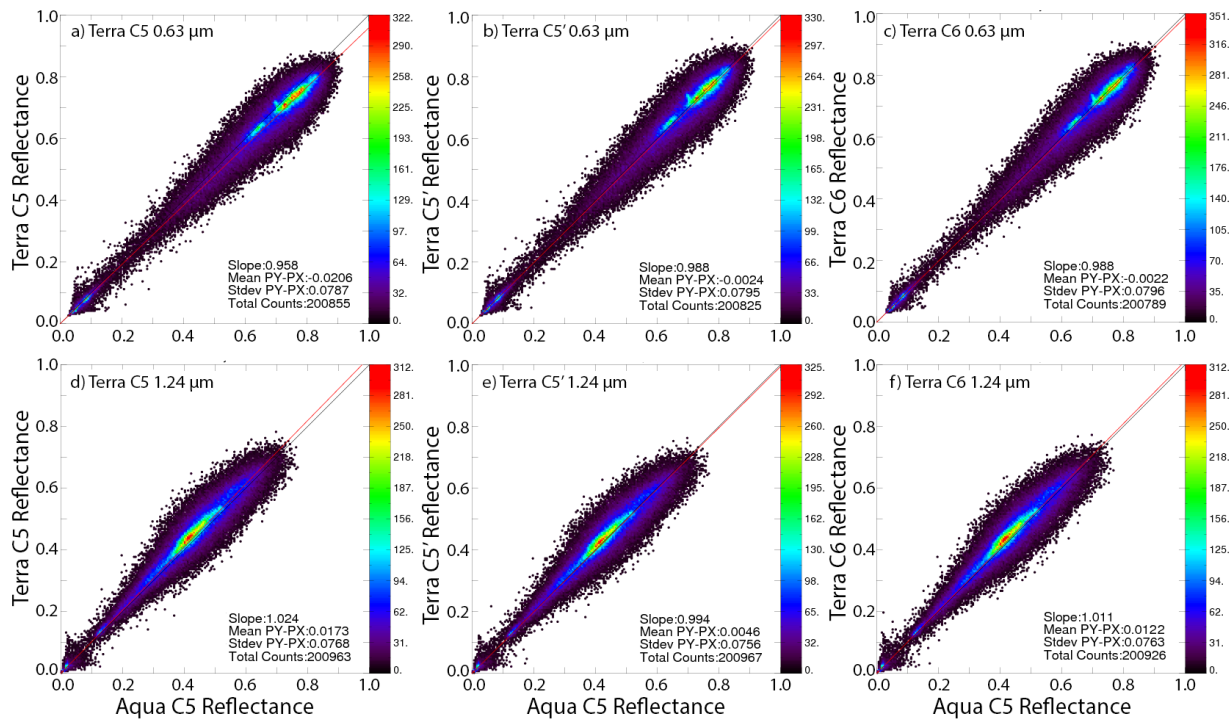


Fig. 2. Reflectance comparisons between matched Terra and Aqua data during 11 April 2015. All Aqua data on the x-axes are C5 reflectances at the same wavelengths as the Terra data. Colors indicate number of 50-km pixels averages for each reflectance pair. Data on y-axes are Terra (a) C5 0.63- $\mu\text{m}$ , (b) adjusted C5, C5', 0.63- $\mu\text{m}$ , (c) C6 0.63- $\mu\text{m}$ , (d) C5 1.24- $\mu\text{m}$ , (e) C5' 1.24- $\mu\text{m}$ , and (f) C6 C5 1.24- $\mu\text{m}$  data. Slope is for force-fit (red) line through origin. PX and PY are the mean Aqua and Terra reflectances, respectively. Stdev is the standard deviation of the differences. The number of samples varies because of differences in meeting the reflectance limits of 0.0 and 1.0.

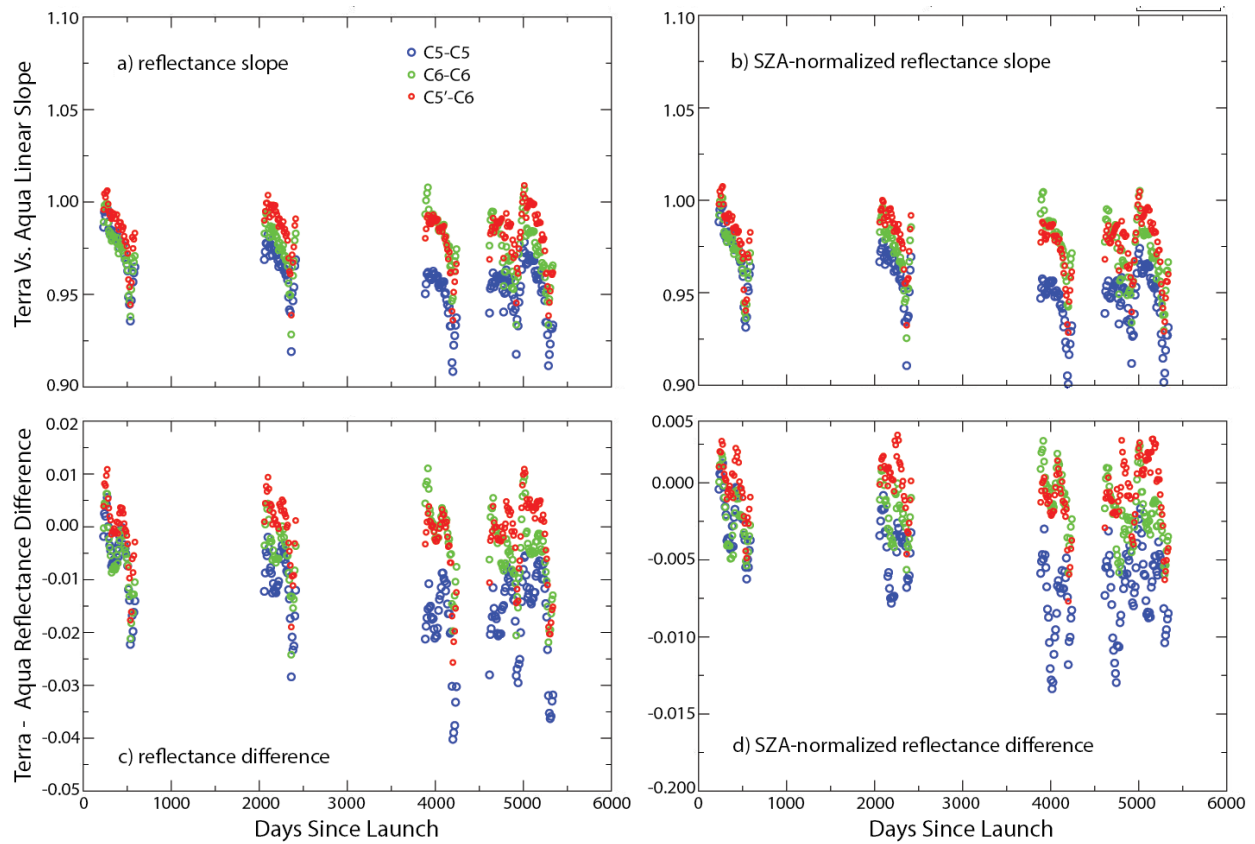


Fig. 3. Daily forced-fit linear slopes (top) and reflectance differences (bottom) for various versions of Terra MODIS collections (C5, C5', and C6) versus Aqua MODIS C5 and C6 reflectances for channel 1 (0.63  $\mu\text{m}$ ) from matched datasets taken days 1, 11, and 21 of each month during 2003, 2008, 2013, 2015, and 2016. Differences are Terra – Aqua. SZA-normalized reflectances are measured reflectances multiplied by the cosine of the solar zenith angle. Days since launch are measured relative to the launch of Aqua, 14 May 2002.

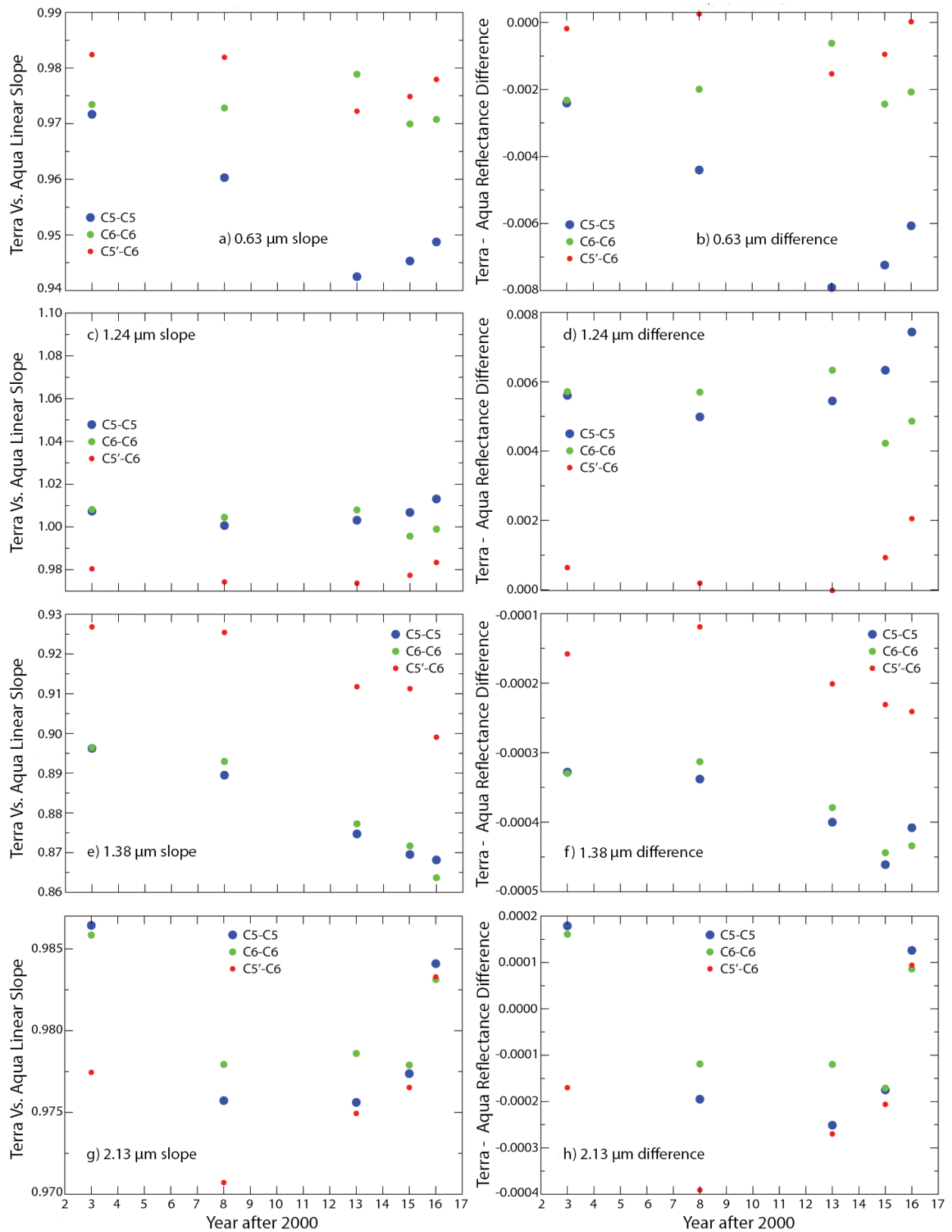


Fig. 4. Annual mean forced-fit linear slopes (left) and reflectance differences (right) for various versions of Terra MODIS collections (C5, C5', and C6) versus Aqua MODIS C5 and C6 reflectances (see Fig. 3) for channels 1 (a,b), 5 (c,d), 26 (e,f), and 7 (g,h) from 36 days of matched datasets taken each year. Differences are Terra – Aqua. All quantities are SZA-normalized.

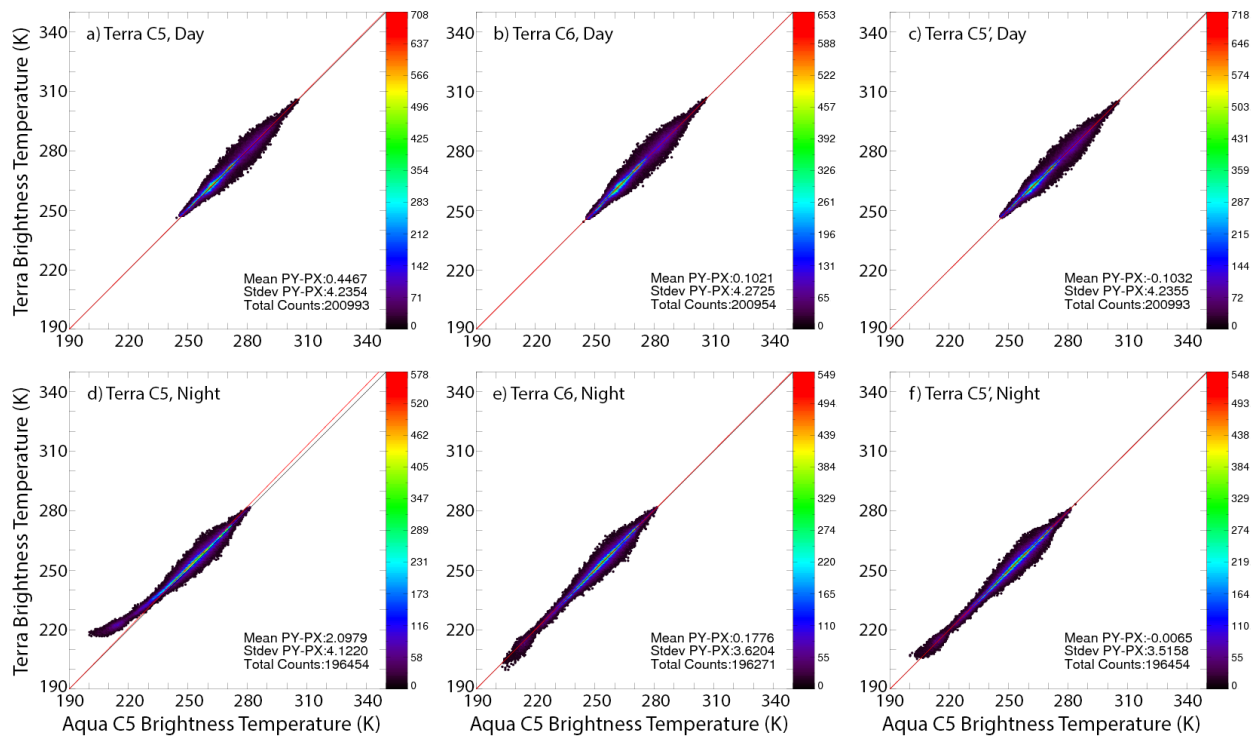


Fig. 5. Same as Fig. 2, except for shortwave infrared (3.8 μm) brightness temperature differences. Top: daytime, bottom: night.



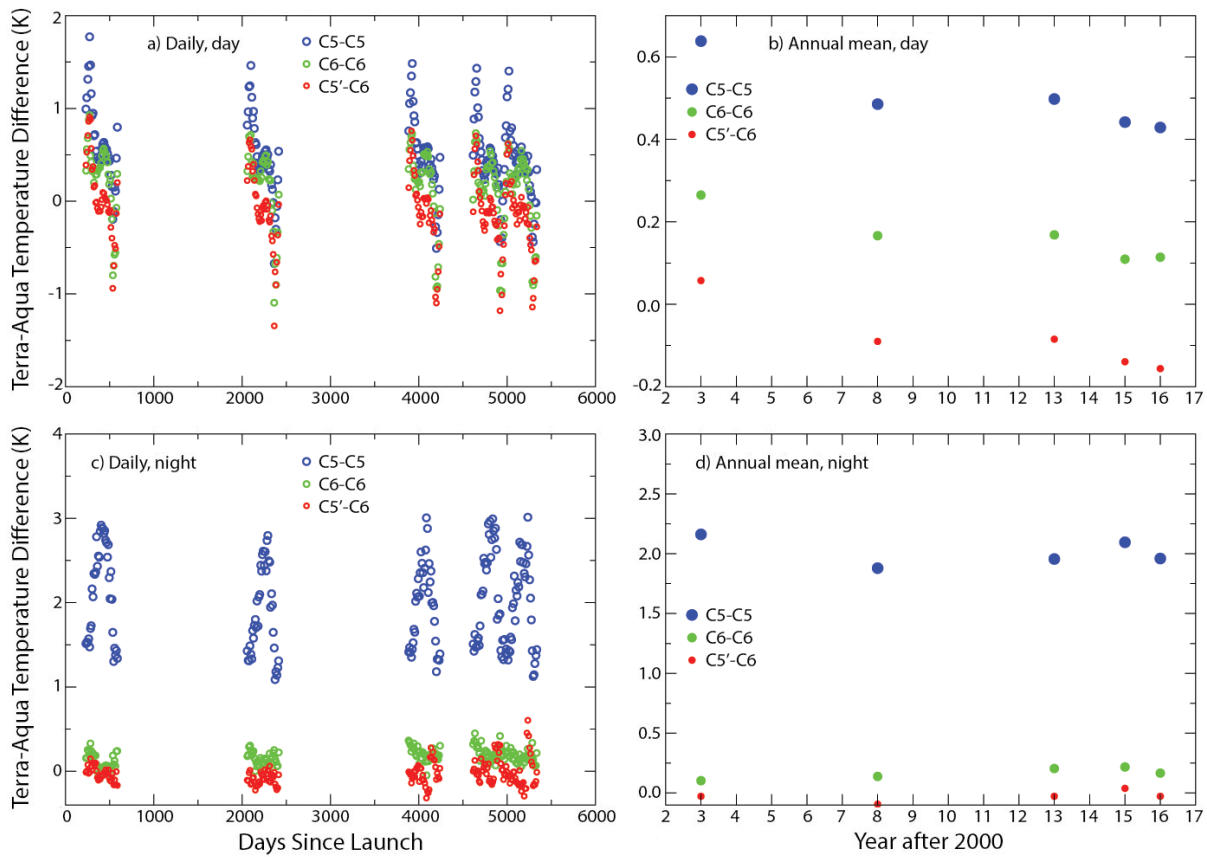


Fig. 6. Daily (left) and annual mean (right) and differences between various versions of Terra MODIS collections (C5, C5', and C6) minus Aqua MODIS C5 and C6 brightness temperatures (see Fig. 3) for channel 20 (3.8  $\mu\text{m}$ ) from 36 days (top) and nights (bottom) of matched datasets taken each year. All differences are Terra – Aqua.

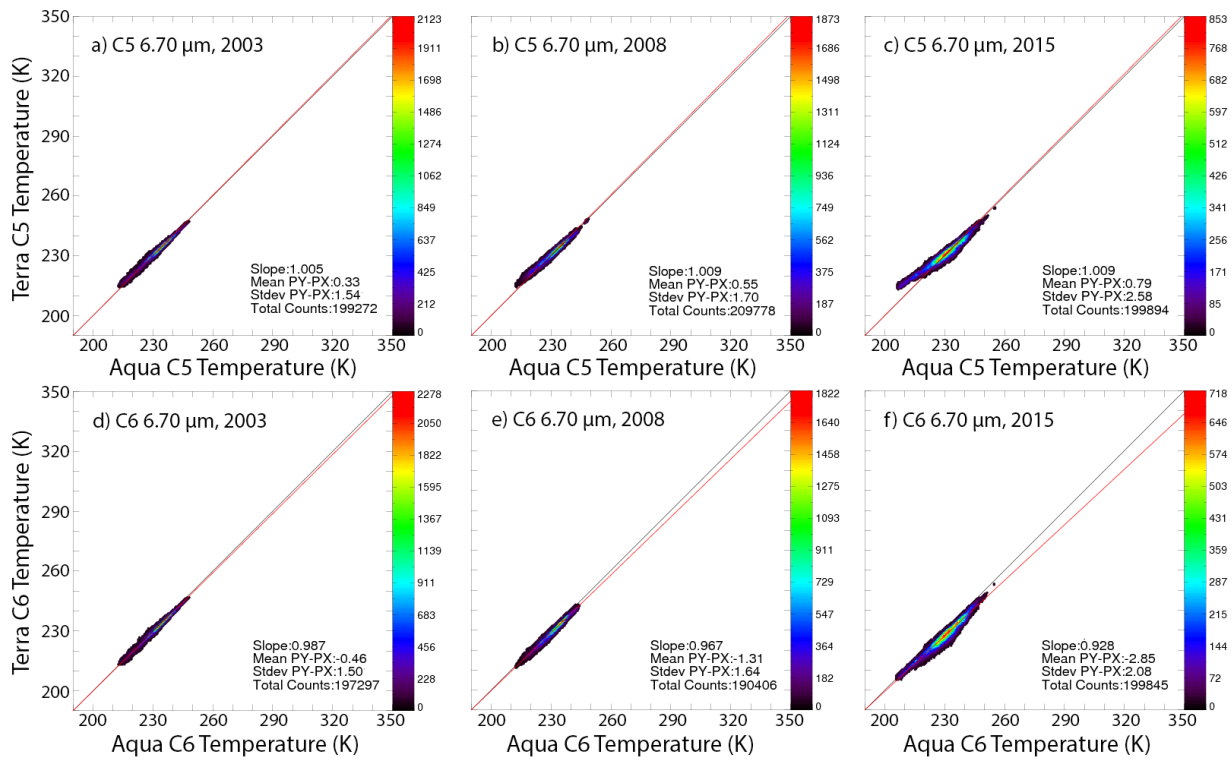


Fig. 7. Channel 27 brightness temperature comparisons between matched Terra and Aqua data at night during 11 July for three different years. Top: C5 data, bottom: C6 data.

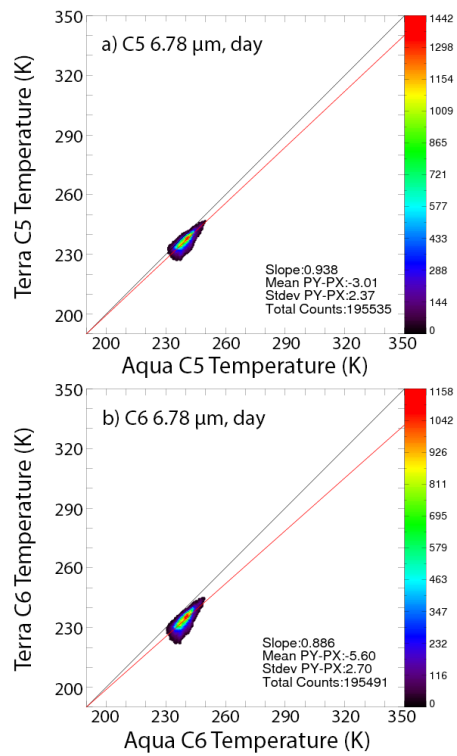


Fig. 8. Channel 27 brightness temperature comparisons between matched Terra and Aqua data in daytime during 11 July 2015. (a) C5 data, (b) C6 data.

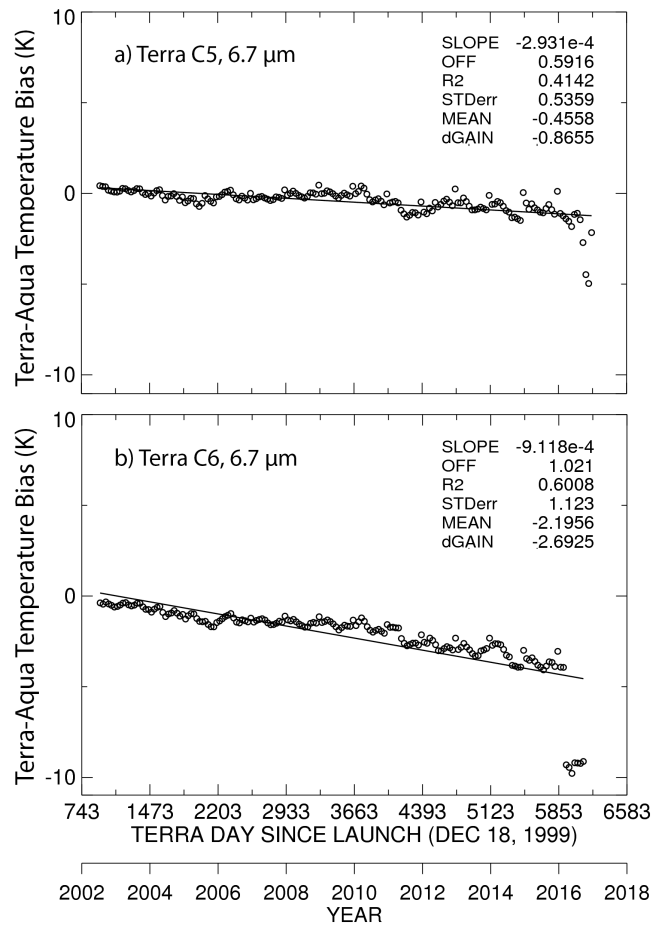


Fig. 9. Channel 27 monthly mean brightness temperature differences between matched Terra and Aqua data. (a) C5 data. (b) C6 data.

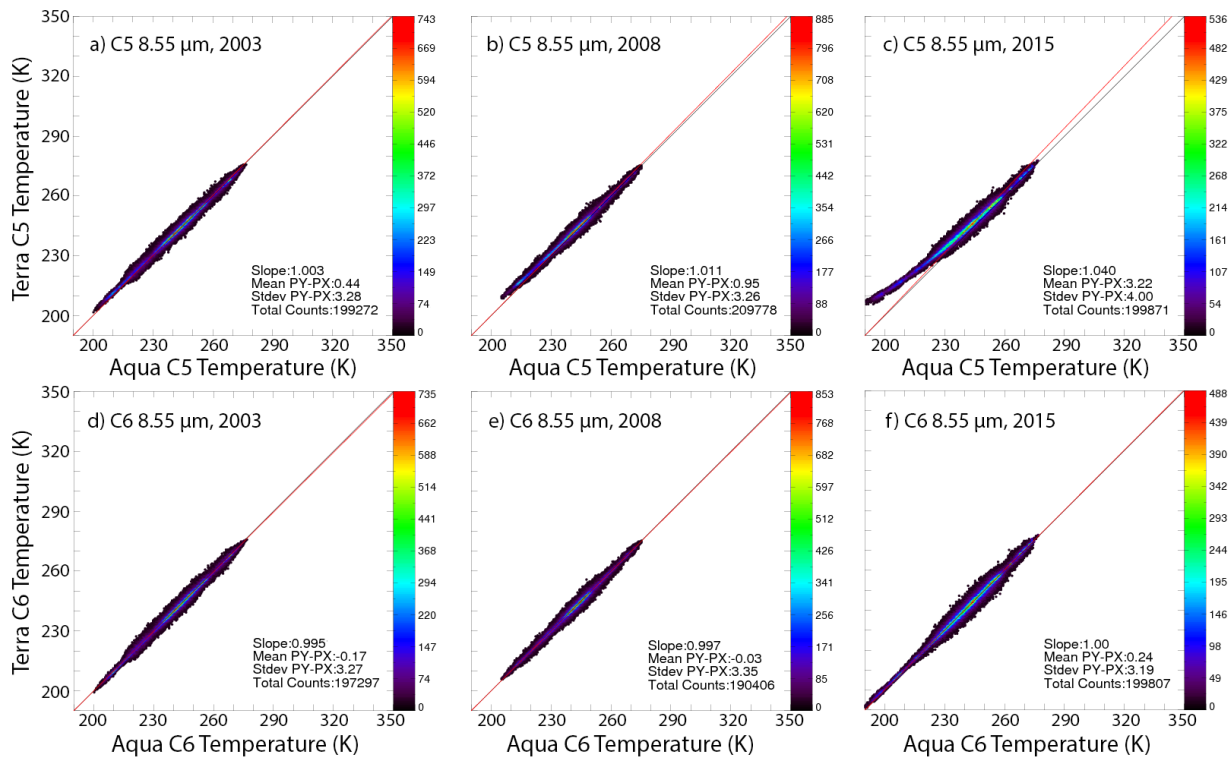


Fig. 10. Same as Fig. 7, except for Channel 29.

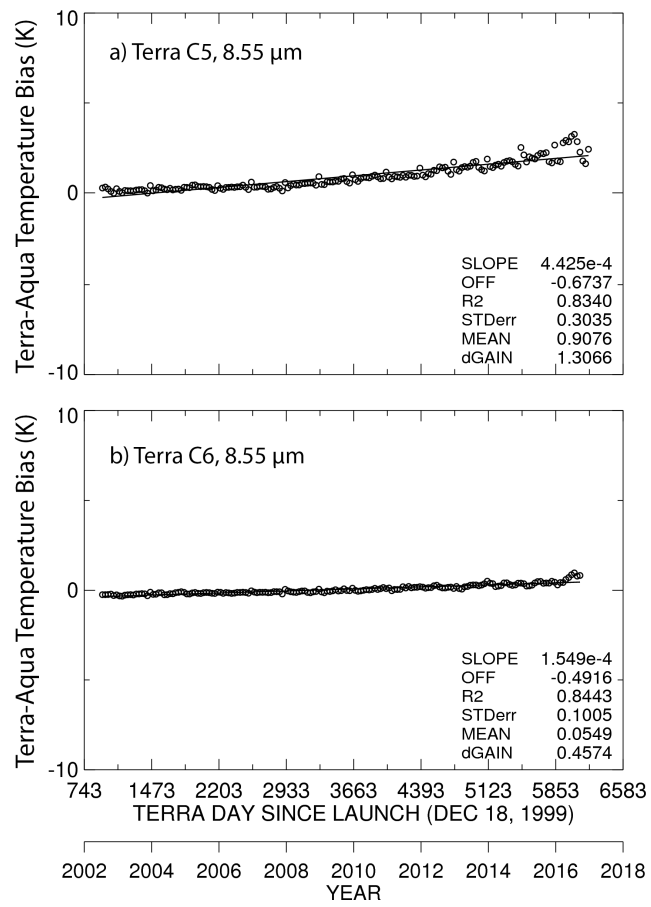


Fig. 11. Same as Fig. 9, except for MODIS channel 29.

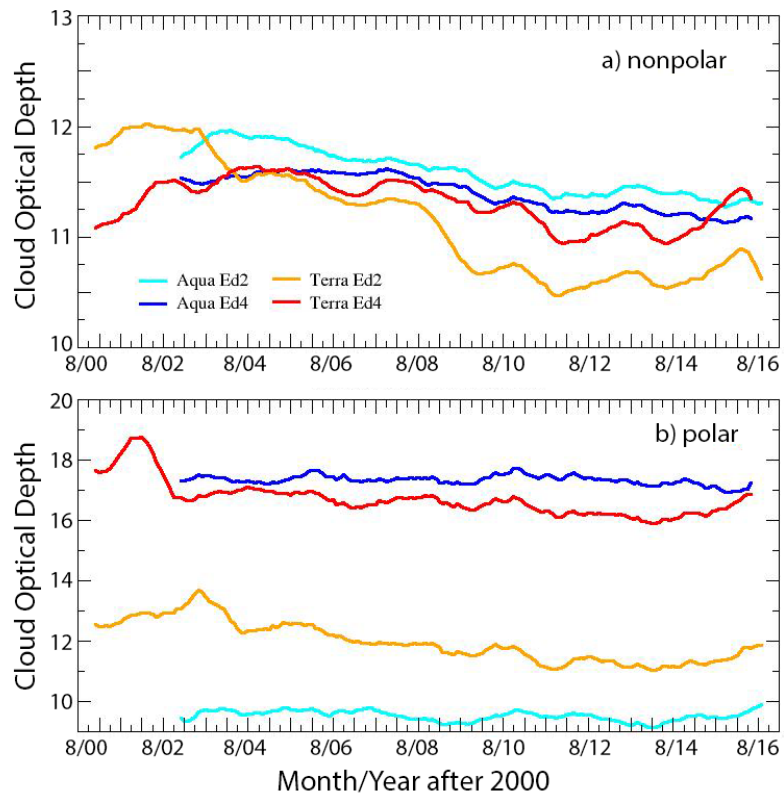


Fig. 12. Twelve-month running mean daytime cloud optical depths from CERES-MODIS retrieval algorithms.

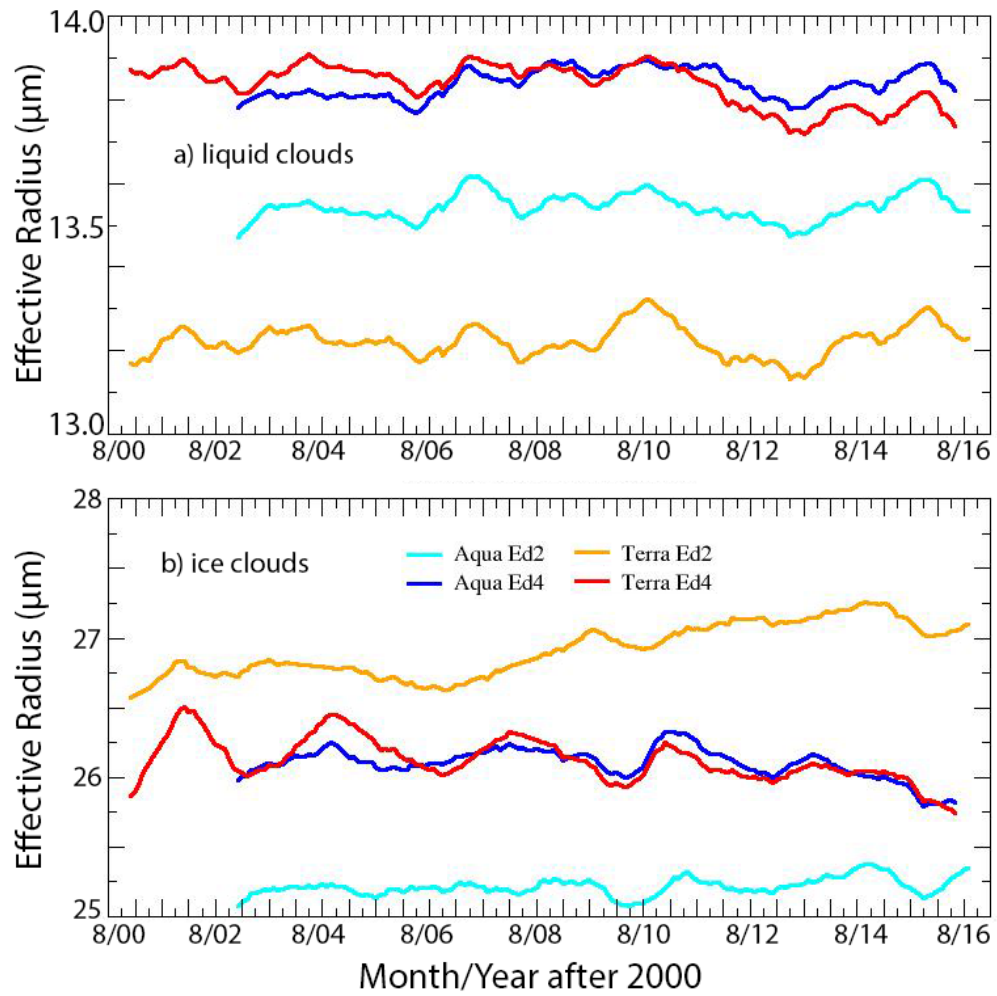


Fig. 13. Same as Fig. 12, except for daytime non-polar particle effective radius.



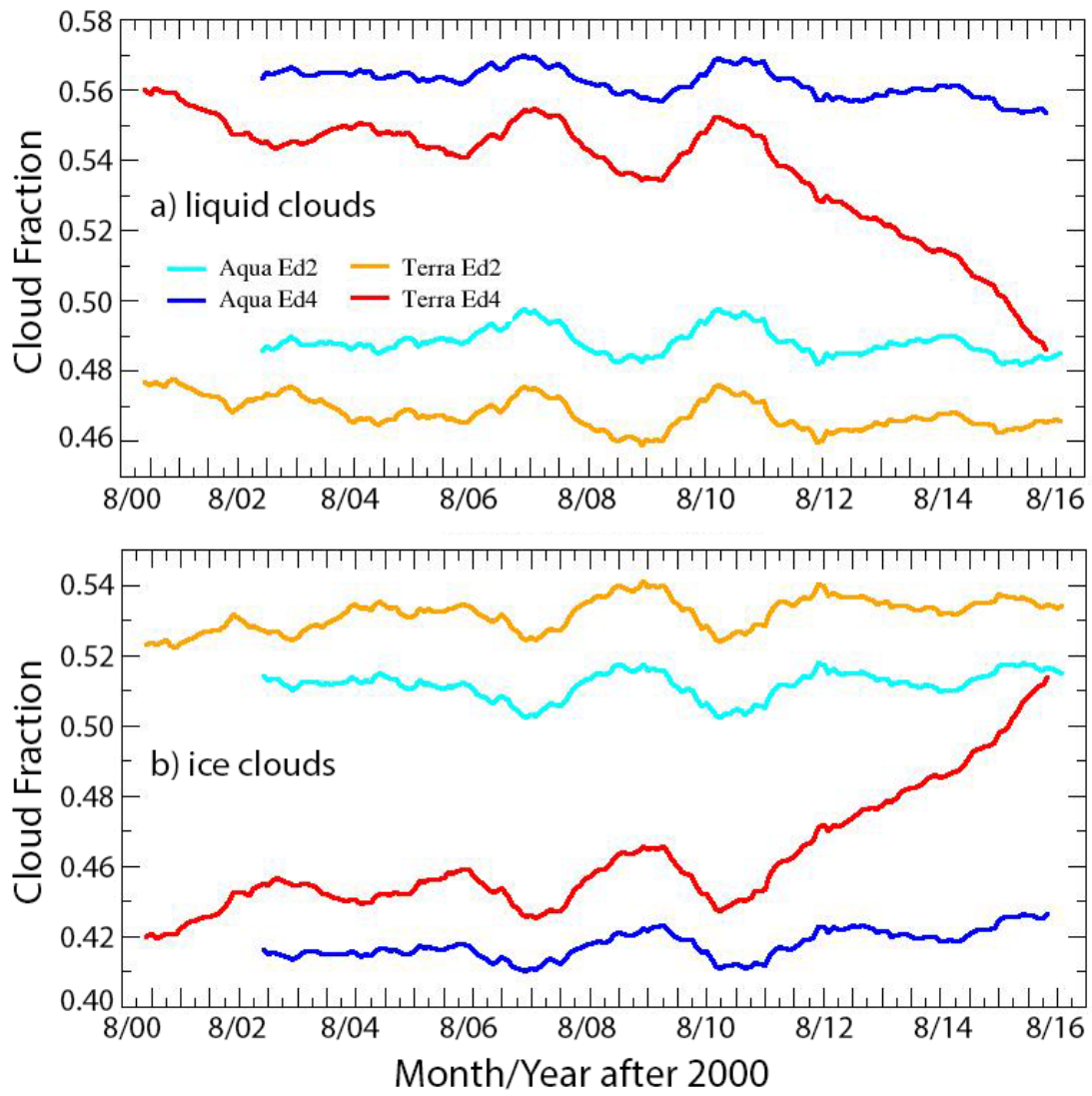


Fig. 14. Same as Fig. 12, except for nighttime cloud phase over non-polar regions.